JOC Article

Hydrolysis of 8-Quinolyl Phosphate Monoester: Kinetic and Theoretical Studies of the Effect of Lanthanide Ions

Bruno S. Souza,[†] Tiago A. S. Brandão,[†] Elisa S. Orth,[†] Ana C. Roma,[‡] Ricardo L. Longo,[‡] Clifford A. Bunton,[§] and Faruk Nome*[,†]

Departamento de Química, Universidade Federal de Santa Catarina, Florianópolis, Santa Catarina, 88040-900, Brazil, Departamento de Química Fundamental, Universidade Federal de Recife, Pernambuco, 50740-540, Brazil, and Department of Chemistry and Biochemistry, University of California, Santa Barbara, California, 93106-9510

faruk@qmc.ufsc.br

Received August 21, 2008

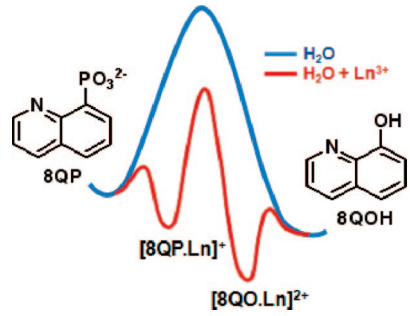

8-Quinolyl phosphate (8QP) in the presence of the trivalent lanthanide ions (Ln = La, Sm, Eu, Tb, and Er) forms a $[Ln \cdot 8QP]^+$ complex where the lanthanide ion catalyzes hydrolysis of 8QP. In reactions with Tb^{3+} or Er^{3+}, there is evidence of limited intervention by a second lanthanide ion. Rate constants are increased by more than 10^7-fold, and kinetic data and B3LYP/ECP calculations indicate that the effects are largely driven by leaving group and metaphosphate ion stabilization. The lanthanides favor a single-step $\mathbf{D_NA_N}$ mechanism with a dissociative transition state, with limited nucleophilic assistance, consistent with the low hydroxide ion dependence and the small kinetic effect of Ln^{3+} radii.

Introduction

Phosphoryl transfer is very important in the control of biological activity,[1,2] notably with very slow phosphate monoester spontaneous hydrolysis, that occur in seconds when catalyzed by kinases or phosphatases.[3] This remarkable acceleration of reactions with poor leaving groups, e.g., alcohol and sugar derivatives, involves precisely located metal ions. Mechanistic differences are striking as compared with reactions in aqueous solution, where in many instances it has been suggested that unlike strictly "dissociative" reactions, enzyme catalysis involves metaphosphate ion-like transition states, with large amounts of bond breaking, and metal ions and cationic side chains should favor the increased negative charge in the transition state.[3−5]

SCHEME 1

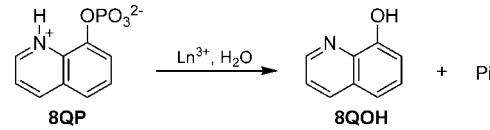

Reactions of dianionic phosphate esters, whose leaving groups contain strongly electron-withdrawing substituents, are often written as involving "dissociation", to the very labile metaphosphate ion, PO_3^-, which should be rapidly trapped by a nucleophilic solvent, e.g., H_2O, present in the substrate's solvent shell. In some reactions, an intermediate can be trapped without affecting the reaction rate, but absent such evidence, the

* Corresponding Author. Tel: +55-48-37216849. Fax: +55-48-37216850.
[†] Universidade Federal de Santa Catarina.
[‡] Universidade Federal de Pernambuco.
[§] University of California.

(1) Barford, D.; Das, A. K.; Egloff, M. P. *Annu. Rev. Biophys. Biolmol. Struct.* **1998**, *27*, 133–164.
(2) Jackson, M. D.; Denu, J. M. *Chem. Rev.* **2001**, *101*, 2313–2340.
(3) Williams, N. H. *Biochim. Biophys. Acta* **2004**, *1697*, 279–287.
(4) Lahiri, S. D.; Zhang, G.; Dunaway-Mariano, D.; Allen, K. N. *Science* **2003**, *299*, 2067–2071.
(5) Cleland, W. W.; Hengge, A. C. *Chem. Rev.* **2006**, *106*, 3252–3278.

10.1021/jo801870v CCC: $40.75
Published on Web 12/24/2008

distinction between "associative" and "dissociative" depends on indirect evidence, for example, by drawing a distinction between substrate solvation and partial formation of a new covalency, relaying on theoretical modeling to make this distinction, or by estimating life times of putative intermediates.

We use the term dissociative to indicate that there is significant P−O1 bond breaking in the transition state. Insofar as water is omnipresent it is difficult to draw a clear distinction between solvation and formation of a new covalent bond. There are many examples of attempts to make this distinction by using ab initio/DFT calculations, and a variety of mechanistic routes are available for the different phosphate derivatives. Triesters such as *O,O*-diethyl *p*-nitrophenyl phosphate (paraoxon) and related compounds react with hydroxide ion and other nucleophiles via rate-limiting pentacoordinate intermediate formation.[6−8] Similarly, the reaction of dineopentyl phosphate anion diester with water proceeds through an associative mechanism which results in a phosphorane intermediate.[9] Simple models of phosphate ester monoanions show that both associative and dissociative mechanisms are represented on the potential energy surface, and the associative mechanism seems to be preferred for metallo-enzymes, while enzymes that function without a metal may react via a dissociative path.[10] Phosphate monoester dianions show a flat potential energy surface for the associative and dissociative mechanisms, and the transition state changes from associative to dissociative upon a decrease in the pK_a of the leaving group.[11,12]

Models sharing enzymic characteristics have shown how catalysis may involve multiple interactions, as in the metallo-phosphatase associative mechanisms.[13−15] Recently, lanthanide ions have shown very strong catalytic efficiencies due to their higher charge densities and coordination numbers than other metal ions, including some with biological relevance,[15,16] and lanthanide ion catalysis is important in synthetic organic chemistry, especially for slow or regioselective reactions.[17,18]

Lanthanide ion complexes are medicinally important, e.g., as magnetic resonance imaging contrast agents,[19,20] luminescent probes,[21−23] and artificial phosphatases, nucleases, and ribonucleases.[24−26] They are potentially useful in detoxification of pesticides and chemical warfare nerve agents.[15,27,28]

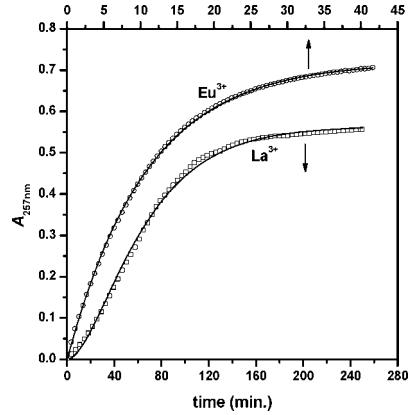

FIGURE 1. Absorbances at 257 nm (A_{257nm}) as a function of time in the hydrolysis of 8QP (33.3 μM) in the presence of 1.28 mM of La^{3+} (□) or 0.98 mM of Eu^{3+} (○). Reactions at pH 7.00, 0.01 M BTP at 25.0 °C. Absorbances were set to zero at time = 0.

Catalysis by Ln^{3+} of phosphate monoester reactions are models for phosphoryl transfer and molecular recognition in biological systems, and in this respect, 8-quinolyl phosphate, 8QP, is a useful substrate in investigating metal ion effects on dephosphorylation of phosphomonoesters. For example, there is a 10^6-fold rate enhancement in the Cu^{2+}-catalyzed hydrolysis of 8QP due to a favorable interaction with oxygen in the leaving group, and in some of these reactions there is high nucleophilicity of metallo-bound H_2O.[29,30] Here, we show effects of trivalent lanthanide ions, Ln^{3+} = La, Sm, Tb, Eu, and Er, on the hydrolysis of 8QP (Scheme 1) and we compare the conclusions with those from B3LYP/ECP calculations.

Results and Discussion

Kinetic and Product Studies. Addition of an excess of any of the trivalent lanthanide ions (Ln = La, Sm, Eu, Tb, and Er) results in fast complexation with 8QP, and the complexed organic phosphate subsequently hydrolyzes. The complexation step for the lanthanide ions was much faster than subsequent hydrolysis, and typical first-order plots were observed for absorbances as a function of time (Figure 1). Reactions of 8QP in the presence of the trivalent lanthanide ions were followed by measuring the absorbance at 257 nm and reactions are first order, except for La^{3+}, where with $[La^{3+}]/[8QP] < 40$ the initial complex formation affects the initial part of the kinetics, but they can be conveniently treated as consecutive first-order reactions (Figure 1). The reaction gives 8-quinolinol (8QOH), or its anion, and inorganic phosphate, identified by absorption and NMR spectroscopy, with comparisons with the spectra of standard samples.[31]

(6) Zheng, F.; Zhang, C. G.; Ornstein, R. L. *J. Chem. Soc., Perkin Trans. 2* **2001**, *12*, 2355–2363.
(7) Bhattacharya, S.; Vemula, P. K. *J. Org. Chem.* **2005**, *70*, 9677–9685.
(8) Kumar, V. P.; Ganguly, B.; Bhattacharya, S. *J. Org. Chem.* **2004**, *69*, 8634–8642.
(9) Kamerlin, S. C. L.; Williams, N. H.; Warshel, A. *J. Org. Chem.* **2008**, *73*, 6960–6969.
(10) Kamerlin, S. C. L.; Wilkie, J. *Org. Biomol. Chem.* **2007**, *5*, 2098–2108.
(11) Klähn, M.; Rosta, E.; Warshel, A. *J. Am. Chem. Soc.* **2006**, *128*, 15310–15323.
(12) Iche-Tarrat, N.; Ruiz-Lopez, M.; Barthelat, J.-C.; Vigroux, A. *Chem.—Eur. J.* **2007**, *13*, 3617–3629.
(13) Holmes, R. R. *Acc. Chem. Res.* **2004**, *37*, 746–753.
(14) Mitić, N.; Smitgh, S. J.; Neves, A.; Guddat, L. W.; Gahan, L. R.; Schenk, G. *Chem. Rev.* **2006**, *106*, 3338–3363.
(15) Schneider, H.-J.; Yatsimirsky, A. K. *The Lanthanides and Their Interrelations with Biosystems*; New York, 2003; Vol. 40, pp 369−462.
(16) Williams, N. H.; Takasaki, B.; Wall, M.; Chin, J. *Acc. Chem. Res.* **1999**, *32*, 485–493.
(17) Marks, T. J.; Hong, S. *Acc. Chem. Res.* **2004**, *37*, 673–686.
(18) Tosaki, S.; Tsuji, R.; Ohshima, T.; Shibasaki, M. *J. Am. Chem. Soc.* **2005**, *127*, 2147–2155.
(19) Zhou, J.; van Zijl, P. C. M. *Prog. Nucl. Magn. Reson. Spectrosc.* **2006**, *48*, 109–136.
(20) Aime, S.; Crich, S. G.; Gianolio, E.; Giovenzana, G. B.; Tei, L.; Terreno, E. *Coord. Chem. Rev.* **2006**, *250*, 1562–1579.
(21) Pandya, S.; Yu, J.; Parker, D. *J. Chem. Soc., Dalton Trans.* **2006**, 2757–2766.
(22) Hemmilä, I.; Laitala, V. J. *J. Fluoresc.* **2005**, *15*, 529–542.
(23) Song, J.-L.; Lei, C.; Mao, J.-G. *Inorg. Chem.* **2004**, *43*, 5630–5634.
(24) Zhu, B.; Xue, D.; Wang, K. *Biometals* **2004**, *17*, 423–433.
(25) Liu, C.; Wang, M.; Zhang, T.; Sun, H. *Coord. Chem. Rev.* **2004**, *248*, 147–168.
(26) Chang, C. A.; Wu, B. H.; Duan, B. Y. *Inorg. Chem.* **2005**, *44*, 6646–6654.
(27) Yang, Y.-C. *Acc. Chem. Res.* **1999**, *32*, 109–115.
(28) Yang, Y.-C.; Baker, J. A. *Chem. Rev.* **1992**, *92*, 1729–1743.
(29) Murakami, Y.; Sunamoto, J. *Bull. Chem. Soc. Jpn.* **1971**, *44*, 1827–1834.
(30) Hay, R. W.; Basak, A. K.; Pujari, M. P.; A., P. *J. Coord. Chem.* **1991**, *23*, 43–55.
(31) Sapelli, E.; Brandão, T. A. S.; Fiedler, H. D.; Nome, F. *J. Colloid Interface Sci.* **2007**, *314*, 212–222.

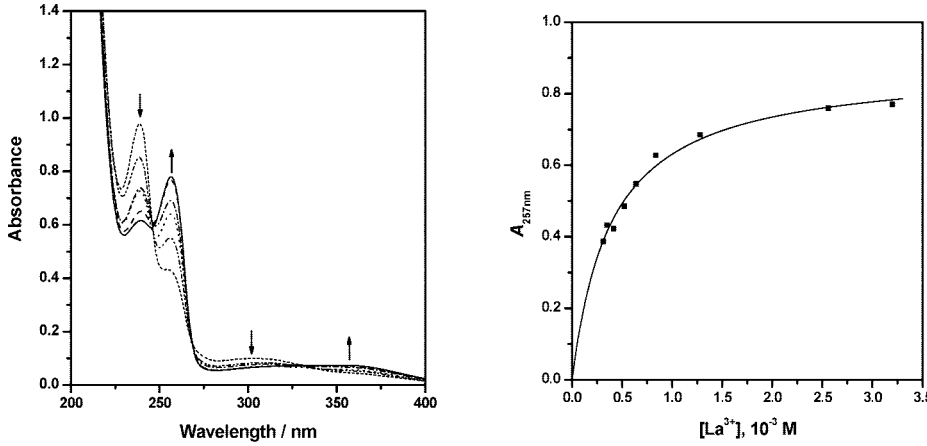

(a) (b)

FIGURE 2. (a) UV−vis spectra of $8QO^-$ in the presence of 0.32 to 3.2 mM [$LaCl_3$], at pH 7.0 and 25 °C. (b) Absorbances of $[La8QO]^{2+}$ complex at 257 nm (A_{257nm}) as a function of [$LaCl_3$], at pH 7.00, 0.01 M BTP and 25 °C. The solid line is a fit by using eq 1.

SCHEME 2

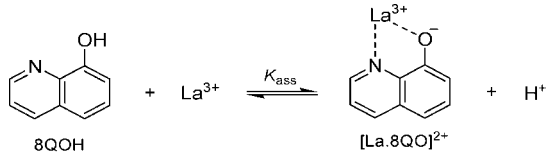

The reaction products are complexes of Ln^{3+} and $8QO^-$ as shown by their spectra, which were identical to those obtained from 8QOH titration with Ln^{3+}. Figure 2a shows the UV−vis spectra taken after at least 8 half-lives of the hydrolysis of 8QP in the presence of different La^{3+} concentrations, and there is a pronounced spectral change as a function of $[La^{3+}]$, consistent with a 1:1 equilibrium complexation of 8QOH with La^{3+} (Figure 2b). Complex formation decreases the pK_a of the hydroxyl group in 8QOH and allows formation of a stronger chromophore ($[La8QO]^{2+}$) and increasing absorbance. The spectral changes reflect the equilibrium depicted in Scheme 2 with derivation of eq 1 and describe observed absorbance changes.

$$A_{257nm} = \frac{A_{Ln8QO} K^{\circ}_{assoc} K_a [Ln^{3+}]_0}{K^{\circ}_{assoc} K_a [Ln^{3+}]_0 + K_a + [H^+]} \qquad (1)$$

For the other lanthanides, the observed behavior was similar to that of La^{3+}. The thermodynamic association constants between 8QOH and Ln^{3+} (K°_{assoc}) were obtained by nonlinear fitting of the absorbance at 257 nm (A_{257nm}) versus $[Ln^{3+}]$ data by using eq 1, where A_{Ln8QO} is the maximum absorbance of the complex and K_a is the 8QOH dissociation constant (2.40×10^{-7})[32] as shown in Table 1.

The observed spectra indicate that ligand−Ln^{3+} bonds have significant ionic character rather than the usual charge-transfer coordination of these ligands with transition-metal ions, and as a consequence, the spectra in the presence of Ln^{3+} are similar to that of 8-quinolinate ion ($8QO^-$).[31] Stability constants for complexes of $8QO^-$ with a variety of lanthanides and metal ions have been estimated and are fully consistent with our results[32] and indicative of strong interactions of Ln^{3+} with the aryl oxide ion.

TABLE 1. K°_{assoc} **and Absorbance Values for the [Ln·8QO]$^{2+}$ complex at 257 nm, pH 7.00, 0.01 M BTP and 25.0 °C**

Ln^{3+}	log (K°_{assoc}, M^{-1})[a]	A_{Ln8QO}
La	6.24 ± 0.01	0.879 ± 0.009
Sm	6.55 ± 0.01	1.019 ± 0.006
Eu	6.93 ± 0.02	0.963 ± 0.017
Tb	6.92 ± 0.02	0.867 ± 0.008
Er	7.25 ± 0.04	0.791 ± 0.014

[a] K°_{assoc} values were corrected according to the free Ln^{3+} fraction.[33]

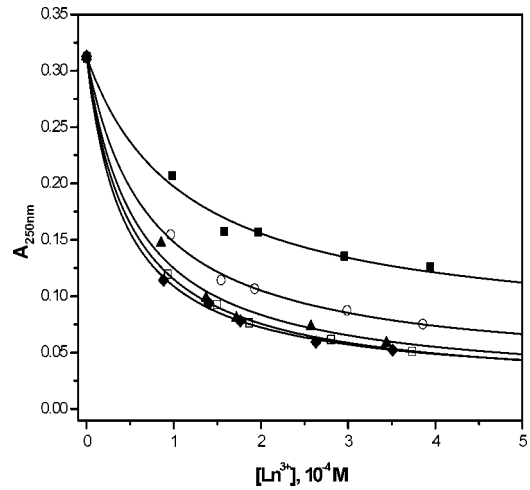

FIGURE 3. Absorbance at 250 nm of 8QP in the presence of (■) $LaCl_3$, (○) $SmCl_3$, (▲) $EuCl_3$, (□) $TbCl_3$, and (◆) $ErCl_3$, at pH 7.0 and 25 °C. Solid lines calculated using eq 2.

In order to determine the association constant between 8QP and the lanthanides ions, the UV−vis spectrum of the mixture was registered immediately after fast mixing in order to minimize spectral changes due to hydrolysis. Increasing the metal ion concentration (for all the lanthanides) decreased the absorbance at 250 nm (Figure 3).

The observed absorbance changes (Figure 3) are consistent with a 1:1 complex between 8QP and the Ln^{3+} (Scheme 3), which allows the derivation of eq 2. Increasing the metal ion concentration decreases the absorbance at 250 nm, allowing

(32) Martell, A. E.; Smith, Z. M.; Motekaitis, R. J. *NIST Critical Stability Constants of Metal Complexes Database: NIST Standard Reference Database 46*; NIST: Gaithersburg, 1993.
(33) Gómez-Tagle, P.; Yatsimirsky, A. K. *Inorg. Chem.* **2001**, *40*, 3786–3796.

SCHEME 3

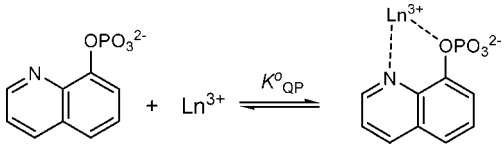

TABLE 2. K_{QP}, K°_{QP}, A_{Ln8QP}, and A_{8QP} Values for the $[Ln\cdot 8QP]^+$ Complex at 250 nm, pH 7.00, 0.01 M BTP and 25.0 °C

Ln^{3+}	log (K_{QP}, M^{-1})[a]	log (K°_{QP}, M^{-1})[a]	A_{8QP}	A_{Ln8QP}
La	3.96	4.07	0.313 ± 0.004	0.070 ± 0.003
Sm	4.14	4.25	0.313 ± 0.002	0.030 ±0.003
Eu	4.25	4.36	0.313 ± 0.009	0.018 ± 0.011
Tb	4.30	4.41	0.313 ± 0.002	0.016 ± 0.002
Er	4.36	4.47	0.313 ± 0.003	0.020 ± 0.003

[a] K_{QP} values were corrected according to the free Ln^{3+} fraction and are accurate to ± 0.05 units.[33]

determination of the apparent association constants (K_{QP}) by the nonlinear fit of the absorbance at 250 nm (A_{250nm}) versus $[Ln^{3+}]$ data with eq 2, and fitted curves are shown in Figure 3. The thermodynamic association constant for the complex formation (K°_{QP}) was calculated by considering the fraction of the phosphate monoester that is deprotonated at the nitrogen atom (eq 3).

$$A_{250nm} = (A_{Ln8QP}K_{QP}[Ln^{3+}]_0 + A_{8QP})\left(\frac{1}{1 + K_{QP}[Ln^{3+}]_0}\right) \quad (2)$$

$$K^{\circ}_{QP} = K_{QP}/\chi_{QP} \quad (3)$$

In eqs 2 and 3, A_{Ln8QP} and A_{8QP} are absorbances of the complex and that of free 8QP, respectively; $[Ln^{3+}]_0$ is the total metal ion concentration, and χ_{QP} is the mole fraction of 8QP deprotonated at the nitrogen atom. The equilibrium constants K_{QP} and K°_{QP} correspond to the apparent and thermodynamic association constants, respectively, for the equilibrium depicted in Scheme 3. The parameters used in the calculation and the calculated equilibrium constants are in Table 2.

Titration Studies. Potentiometric titrations in the pH range 3−11 gave pK_a values for 8QP of 4.30 ± 0.01 and 6.62 ± 0.02. Spectrophotometric titration was used to assign these pK_a values to hydroxyl or quinolinium groups. Spectral scans from pH 2.0 to 7.8 at 242 and 247 nm (isosbestic point) were used to calculate pK_a values of 4.40 ± 0.03 and 6.48 ± 0.03 (Figure 4a). We observed a smaller absorbance change for the first relative to the second pK_a, indicating that it corresponds to deprotonation of the quinolinium moiety as confirmed by ^{31}P and ^{1}H NMR titrations. As shown in Figure 4b, deprotonation of the phosphate hydroxyl group induced large upfield shifts on the ^{31}P signal, while deprotonation at nitrogen did not. The dependence of ^{1}H chemical shifts on pH shows upfield shifts on H-2 and H-4 signals with phosphate group deprotonation, consistent with interaction of the phosphate dianion with the acidic hydrogen quinolinium atom, in the so-called Proton Sponge effect.[34] This effect shifts the pK_a of the NH^+ group from 4.94 in the 8-hydroxyquinolinium ion[32] to 6.48 in 8QP. Potentiometric titrations at 25 °C of 8QP/Ln^{3+}/BTP mixtures were not possible with lanthanide ions, because of fast hydrolysis of 8QP in their presence, and insolubility of the 8QP-lanthanide complexes prevents titration at low temperature (10 °C).

ATR-FTIR Studies. As a consequence of the ionic nature of ligand−Ln^{3+} bonds, UV−vis spectra of 8QP-Ln^{3+} complexes at pH 7 were indistinguishable from those without Ln^{3+}. Therefore, attenuated total reflectance infrared (ATR-FTIR) spectroscopy is a useful method for product identification but because of the form of the equipment not for kinetic work. It was employed to give evidence on Ln^{3+} complexation with 8QP. Figure 5a shows the spectra for aqueous 8QP and $H_2PO_4^-$/HPO_4^{2-} (Pi) in the absence of La^{3+}, and Figure 5b shows the spectra at the beginning and end of hydrolysis in the presence of La^{3+}.

Without La^{3+}, the Pi vibrational spectrum shown in Figure 5a is formally that of $H_2PO_4^-/HPO_4^{2-}$ at pH 7.0, due to the asymmetric stretching in the PO_3 and PO_3H moieties, as in the literature.[35] Comparison of the 8QP spectrum at pH 9.0 (phosphate moiety as a dianion) with the vibrational frequencies for a series of aromatic phosphate monoester dianions,[36] allows assignment of the bands at 979 and 1107 cm^{-1} to symmetric and asymmetric stretchings in the PO_3 moiety, respectively. Similarly, the peaks at 1142 and 1202 cm^{-1} correspond to C−O and P−O−C stretchings.[37]

Comparatively, the symmetric and asymmetric stretching vibrations of the PO_3 moiety in the La·8QP spectrum are systematically shifted toward lower frequencies from 979 and 1107 cm^{-1} to 914 and 1001 cm^{-1}, respectively, while the C−O band is displaced from 1142 to 1108 cm^{-1}. In addition, there is a broad band at 1151 cm^{-1} that can also be assigned to the asymmetric stretching vibrations in the PO_3 moiety, probably due to symmetry lowering caused by coordination of the phosphate group with Ln^{3+}. The spectrum at the end of the hydrolysis reaction is basically identical with the La·Pi vibrational spectrum at pH 7.0, but the asymmetric vibrations of the PO_3H moiety are missing, due to displacement of hydrogen by La^{3+}, and there is a broadband with a maximum at 1054 cm^{-1} due to asymmetric stretching of the PO_3 moiety. The band at 1104 cm^{-1} due to the 8-quinolinolate C−O stretching is similar to the C−O band of 8QP in the complex with La^{3+} (Figure 5b). The band positions of 8QP and of the products in the presence of the other Ln^{3+} are similar (not shown), with similar vibrational frequencies through the series and are essentially identical to those shown in Figure 5b, because interactions are similar.

The ATR-FTIR spectra were taken as a function of time with approximately equimolar concentrations of 8QP and lanthanide ion. The results show disappearance of the band at 1150 cm^{-1} (asymmetric stretching in the PO_3 moiety of the $[Ln\cdot 8QP]^+$ complex) and appearance of a band at 1050 cm^{-1}, assigned as the asymmetric stretching vibrations of the PO_3 moiety in the $[Ln\cdot PO_4\cdot 8QO]$ complexes (Figure 6). Examples of these spectral changes for La^{3+}, Tb^{3+}, and Er^{3+} are given in Figure S2 of the Supporting Information.

Figure 7 presents the kinetic results for the lanthanide catalyzed hydrolysis of 8QP with respect to $[Ln^{3+}]$ at different pHs in all cases with a significant acceleration. All kinetic

(34) Staab, H. A.; Saupe, T. *Angew. Chem., Int. Ed.* **1988**, *27*, 865–879.

(35) Tejedor-Tejedor, M. I.; Anderson, M. A. *Langmuir* **1990**, *6*, 602–611.

(36) Cheng, H.; Nikolic-Hughes, I.; Wang, J. H.; Deng, H.; O'Brien, P. J.; Wu, L.; Zhang, Z.-Y.; Herschlag, D.; Callender, R. *J. Am. Chem. Soc.* **2002**, *124*, 11295–11306.

(37) Silverstein, R. M.; Webster, F. X. *Spectrometric Identification of Organic Compounds*; John Wiley & Sons: New York, 2005; p 126.

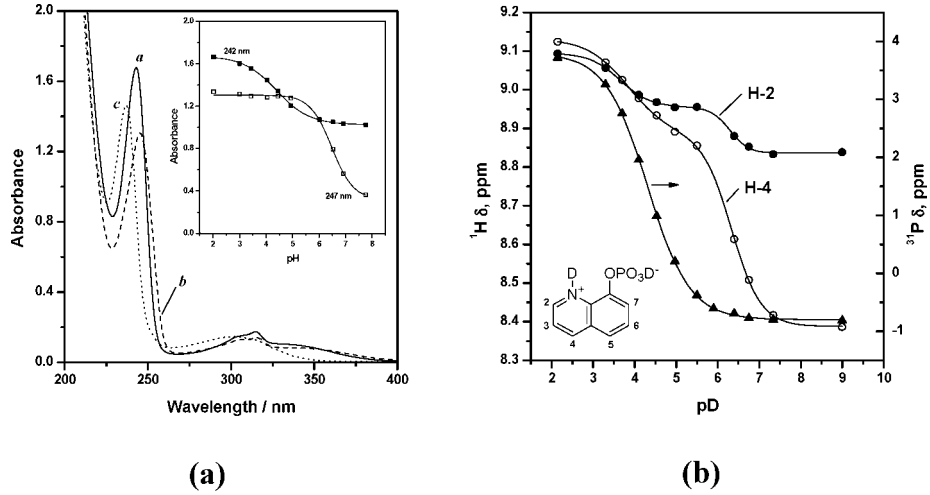

FIGURE 4. (a) Spectrophotometric scans of aqueous 33.3 μM 8QP at pH 2.0 (a), 4.9 (b), and 7.8 (c). The inset corresponds to absorbances at 242 (■) and 247 nm (□) as functions of pH, at 25.0 °C. (b) ^{31}P (▲) and ^{1}H NMR chemical shifts for H-2 (●) and H-4 (○) as a function of pD, 0.04 M 8QP at 25 °C.

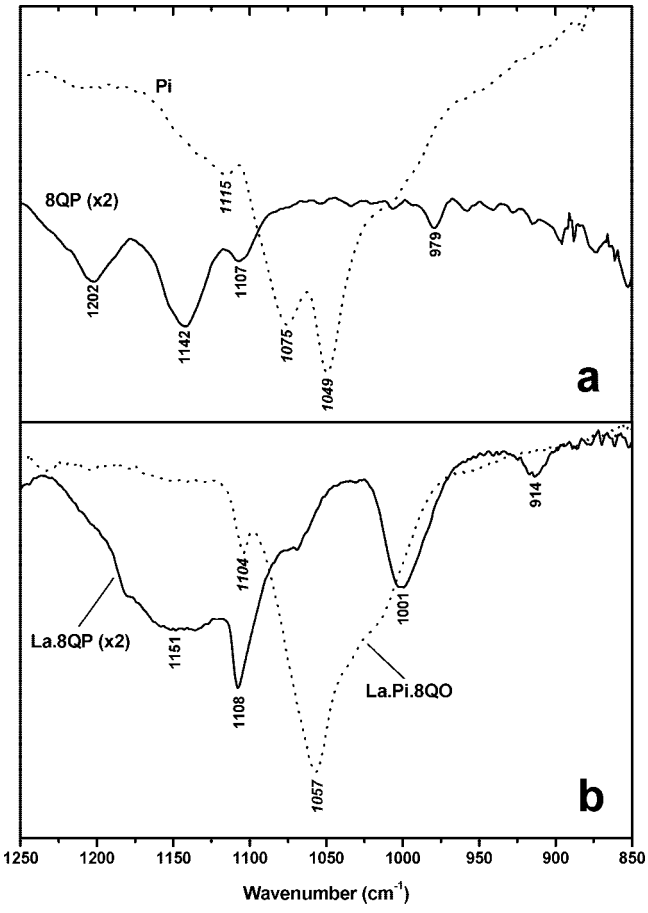

FIGURE 5. ATR-FTIR spectra (in transmittance) of aqueous 1.0 mM 8QP and Na_2HPO_4 (Pi) in the absence of La^3 (a) and at beginning (solid) and end (dotted) of hydrolysis of 1.0 mM 8QP in the presence of 2.0 mM La^{3+} at pH 7.0 (b). The spectra in the presence of La^{3+} were at pH 7.0 and in its absence at pH 9.0 (8QP) and 7.0 (Pi).

experiments were performed in the presence of BTP which, besides acting as a buffer, complexes with Ln^{3+} and, therefore, prevents aggregation and precipitation of the free lanthanide ions.[38]

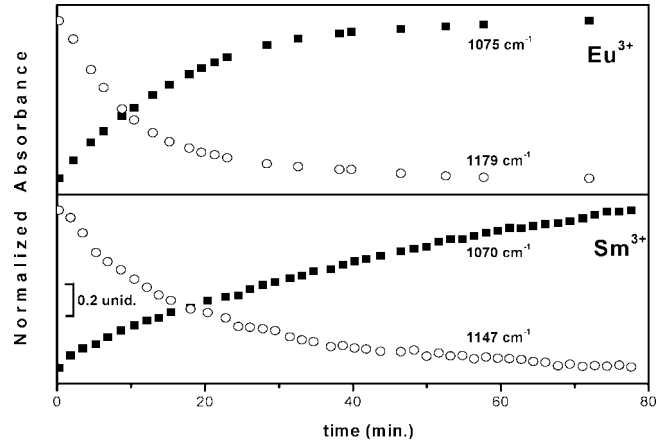

FIGURE 6. Kinetic profile for the hydrolysis of 8QP in the presence of Ln^{3+}; aqueous 1.0 mM 8QP (initial concentration) and 1.0 mM Eu^{3+} and 2.0 mM Sm^{3+} 0.01 M of BTP at 25 °C. The absorbances were normalized in relation to the highest values.

SCHEME 4

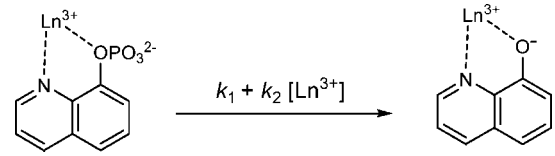

In the lanthanide-mediated hydrolysis of bis(2,4-dinitrophenyl)phosphate (BDNPP), increasing [BTP] from 0.01 to 0.1 M inhibits the reaction, probably because coordination of lanthanide ions with BDNPP is weaker than that with BTP (K_{assoc} = 200 M^{-1}).[39] In the present reaction, an increase in [BTP] in the same range, at pH 8.0, and with 1.0 mM La^{3+} did not affect the hydrolysis of 8QP. This behavior is general[40] and is fully consistent with the fact that the association constant of the lanthanides with this organic substrate (K_{QP}) is at least 2 orders of magnitude larger relative to the BTP−La^{3+} complex (Table 2). Kinetics of the lanthanide catalyzed hydrolyses show two

(38) Longhinotti, E.; Domingos, J. B.; Szpoganicz, B.; Neves, A.; Nome, F. *Inorg. Chem.* **2005**, *358*, 2089–2092.

(39) Longhinotti, E.; Domingos, J. B.; Silva, P. L. F.; Spoganicz, B.; Nome, F. *J. Phys. Org. Chem.* **2005**, *18*, 167–172.

(40) Bruice, T. C.; Tsubouchi, A.; Dempcy, R. O.; Olson, L. P. *J. Am. Chem. Soc.* **1996**, *118*, 9867–9875.

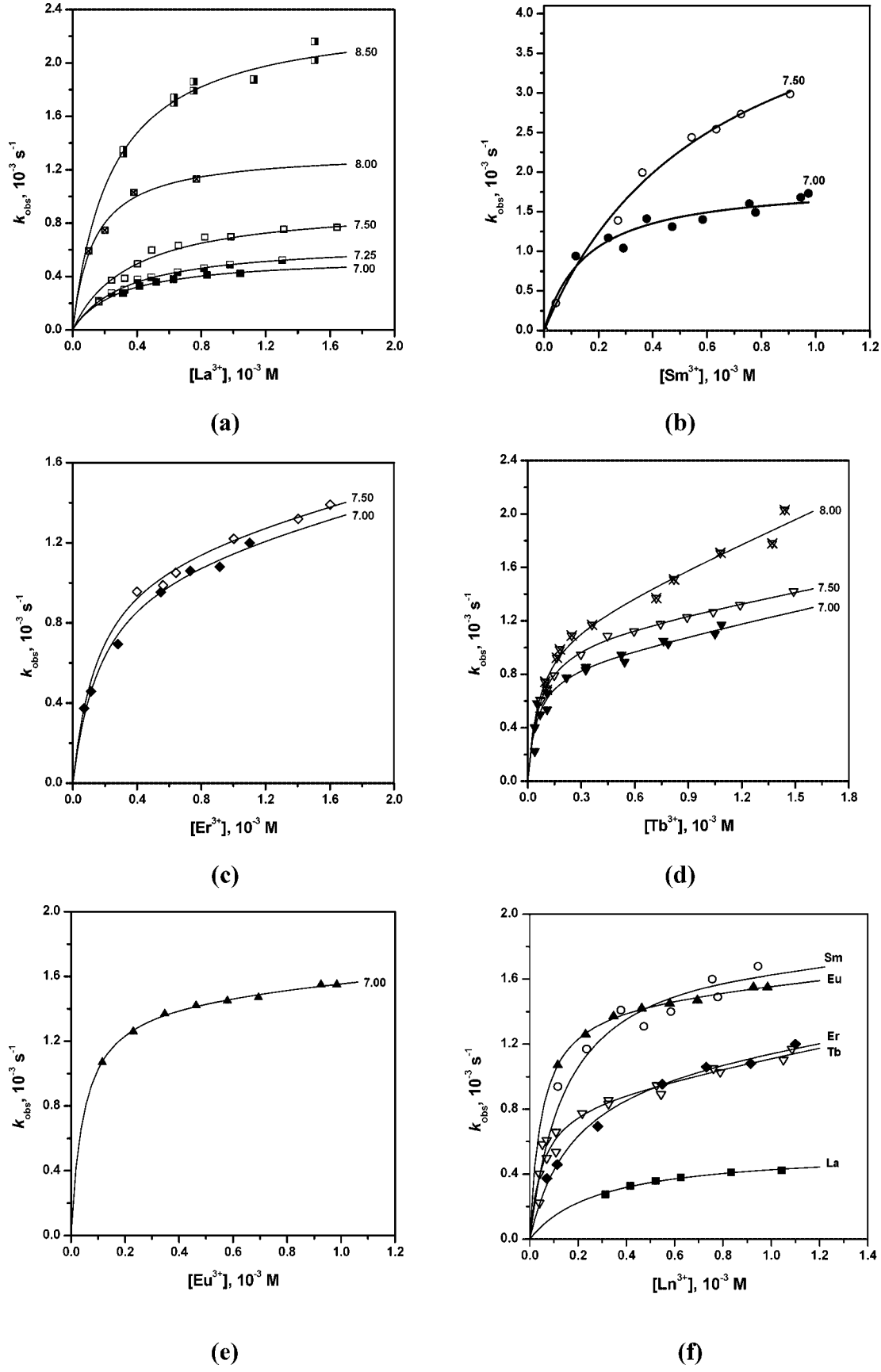

FIGURE 7. (a−e) Variation of k_{obs} for the hydrolysis of 8QP with respect to concentrations of various lanthanides as a function of pH, 0.01 M BTP and 25.0 °C. In (f) are the data for all lanthanides at pH 7.00. The solid lines are fits modeled according to eq 4, with equilibrium and kinetic parameters in Table 3.

TABLE 3. Association and Rate Constants for Hydrolysis of 8QP in the Presence of Ln^{3+} at Different pH, with 0.01 M BTP at 25.0 °C[a]

	pH	$\log(K_{QP}^{kin}, M^{-1})$	$(\chi_{Ln})^b$	$10^4 \times k_1, s^{-1}$	$k_2, M^{-1}s^{-1}$ (%)[c]
La^{3+}	7.00	3.79 ± 0.17	0.986	5.50 ± 0.04	
	7.25		0.970	6.57 ± 0.06	
	7.50		0.945	9.46 ± 0.06	
	8.00		0.832	13.4 ± 0.3	
	8.50		0.582	23.8 ± 0.2	
Sm^{3+}	7.00	3.95 ± 0.19	0.964	16.5 ± 0.3	
	7.50		0.362	50.9 ± 0.7	
Eu^{3+}	7.00	4.36 ± 0.05	0.873	16.5 ± 0.8	
Tb^{3+}	7.00	4.42 ± 0.13	0.924	9.1 ± 0.3	0.26 ± 0.04 (3.0 − 23.5)
	7.50		0.328	10.9 ± 0.1	0.25 ± 0.01 (2.3 − 18.9)
	8.00		0.055	11.5 ± 0.2	0.59 ± 0.06 (4.9 − 34.0)
Er^{3+}	7.00	4.43 ± 0.05	0.678	6.80 ± 0.40	0.55 ± 0.05 (4.0 − 35.0)
	7.50		0.011	9.50 ± 1.5	0.30 ± 0.02 (1.5 − 13.2)

[a] Values of log K_{QP}^{kin} were corrected considering χ_{Ln}. [b] Mole fractions of free Ln^{3+} (χ_{Ln}), obtained from potentiometric titrations of the Ln^{3+}/BTP systems.[33,39] [c] Contribution of k_2 to the overall reaction in the range of 0.1−1 mM [Ln^{3+}].

behaviors, both independent of the presence of BTP: (i) with La^{3+}, Sm^{3+} and Eu^{3+} the reaction follows a classic saturation profile of stoichiometry 1:1 (Ln/8QP); whereas (ii) with Er^{3+} and Tb^{3+}, saturation is followed by a modest linear increase in k_{obs} (Figure 7). The following model, depicted in Scheme 4, is consistent with these observations, which can be expressed as

$$k_{obs} = (k_1 + k_2[Ln^{3+}]_0)\chi_c \quad (4)$$

where χ_c is the mole fraction of the complex given by

$$\chi_c = \frac{K_{QP}^{kin}K_a[Ln^{3+}]_0}{K_{QP}^{kin}K_a[Ln^{3+}]_0 + K_a + [H^+]} \quad (5)$$

where K_a is the acid dissociation constant of the quinolinium group in 8QP, K_{QP}^{kin} is the apparent association constant for complexation of 8QP with Ln^{3+}, and $[Ln^{3+}]_0$ represents the total lanthanide ion concentration. The kinetic parameters obtained by least-squares fits are given in Table 3, and in all cases, the K_{QP}^{kin} values agree with those obtained from the complexation studies (Table 2).

The K_{QP}^{kin} values for the formation of the $[Ln\cdot 8QP]^+$ complex (Table 3) are similar to those determined spectroscopically (Table 2) and are at least 2 orders of magnitude greater than those for the interaction of lanthanides and BTP (vide supra), a fact fully consistent with the lack of an effect of BTP in this particular reaction. In the hydrolysis reactions in the presence of La^{3+}, Sm^{3+}, and Eu^{3+}, the kinetic data can be adequately explained with only the k_1 term. Conversely, in the presence of Tb^{3+} and Er^{3+} there is evidence of a small contribution of the second order term k_2. The percentages of reaction going through the k_2 pathway are given in Table 3, and the contribution of the k_2 term to the overall reaction is significantly smaller than that of k_1. With 0.1 mM Tb^{3+} (or Er^{3+}), the reaction proceeds with a contribution of a second lanthanide ion, which is less than 5% (Table 3). It is important to note that, although in Scheme 4 Ln^{3+} is shown as promoting reaction of the first complex, the reaction may actually correspond to the complexation of 8QP to a dinuclear lanthanide complex, such as those participating in the hydrolysis of BDNPP or BNPP.[33,39] The existence of binuclear polyhydroxo species has been postulated, but there is the difficulty in identifying them as reactive species, and potentiometric titrations by Gómez-Tagle and Yatsimirsky[33] identified $[Eu_2(BTP)_2(OH)_2]^{4+}$ as the main species for Eu^{3+} at pH 7.8 and Longhinotti et al.[39] concluded that for Sm^{3+}, the main species is $[Sm_2(BTP)_2(OH)_5]^+$. However, because under relatively low concentrations of Ln^{3+} (0.1 mM) the monolanthanide complex seems to be the dominant reactive form, and responsible for about 95−99% of the reaction, we focus our studies on it.

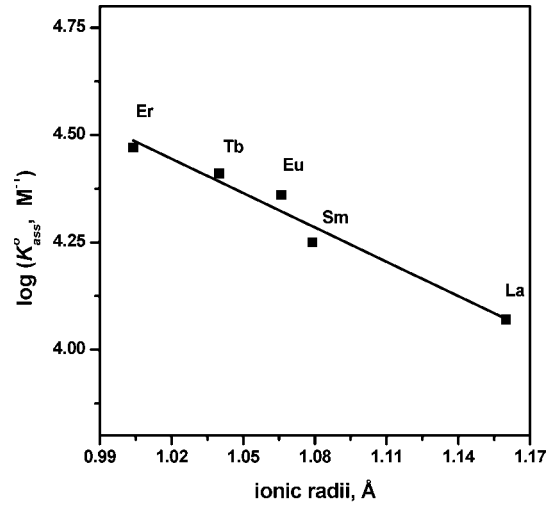

FIGURE 8. Logarithm of thermodynamic association constants for $[Ln\cdot 8QP]^+$ at pH 7.00 as a function of Ln^{3+} radii, 0.01 M BTP at 25.0 °C. Ionic radii for coordination number eight are from Shannon.[41]

While the k_1 values for reaction with the largest lanthanides (La^{3+} and Sm^{3+}) increase monotonically over the pH range, these increases are less significant for the smaller lanthanides, probably because La^{3+} and Sm^{3+} can expand its coordination number with an additional hydroxo ligand as the pH increases, whereas the smaller ions would not have this ability. Figure 8 shows the dependence of the thermodynamic association constant for the complex formation (K°_{assoc}) with respect to the lanthanide radii at pH 7.0. Effects on K°_{assoc} are small, so that log K°_{assoc} increases modestly from La^{3+} to Er^{3+}.

This overall effect is quite general over a number of ligands but it is subject to uncertainties. Basically, the increase of K°_{assoc} with decreasing Ln^{3+} diameter has been ascribed to the higher charge density of the smaller lanthanide ions.[33,42,43] Regarding the steric requirements for complexation of the lanthanides and 8QP, it is known that all lanthanides can form bonds as long as 2.5 Å, which would uniformly allow complexation with the quinolinic nitrogen and the phosphate oxygen

(41) Shannon, R. D. *Acta Crystallogr.* **1976**, *A32*, 751–767.
(42) Moss, R. A.; Jiang, W. *Langmuir* **2000**, *16*, 49–51.
(43) Roigk, A.; Hettich, R.; Schneider, H.-J. *Inorg. Chem.* **1998**, *37*, 751–756.

atoms (vide infra). A probable model for the small effect of the diameter of the lanthanide on the K°_{assoc} values involves solvation and coordination numbers of the Ln^{3+}. Insofar as hydration energies of the lanthanides decrease for the higher coordination numbers, which are ca. 9 for La^{3+} to Eu^{3+} and 8 for those with smaller radii,[44,45] the increasing stability with a larger charge to radius (Z/r) ratio is accompanied by a hydration barrier hindering coordination with 8QP.

The influence of Ln^{3+} radii on k_1 values is small in the pH range studied. Below pH 7.0, the reaction is much slower and the kinetic behavior is complex, most probably because the complexation becomes rate determining and thermodynamically unfavorable (Supporting Information). The observed increase in rate constants follow complexation in solution, and the observed increase in k_1 may be related to formation of monohydroxo [La·8QP(OH)]$^{2+}$ complexes, **1**, as for the hydroxo complexes in the Ln^{3+}/BTP systems.[33,39]

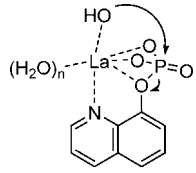

1

The extent of catalysis promoted by the lanthanide ions formally involves the reactivity of $8QP^{2-}$, which is very unreactive without the lanthanides. Although the rate constant for this spontaneous reaction is unknown, it can be predicted, from hydrolyses of 8QP at higher temperatures, to be of the order of 5×10^{-10} s^{-1} at pH 7.0 and 25 °C.[46] Thus, the lanthanide ion causes a greater than 10^7-fold rate enhancement at pH 7.0, which may increase modestly with other Ln^{3+} due to contribution of the k_2 reaction.

A probable factor in the lanthanide acceleration of the hydrolysis of $8QP^{2-}$ is the decrease of the leaving group pK_a (pK_{lg}), which, by assuming k_1 values for La^{3+}, and comparing them to those of phosphate monoesters assigns a leaving group pK_a of about 5.5. Provided that the mechanism promoted by lanthanide ions resembles those in their absence, the catalyzed hydrolysis should have a typical $\mathbf{D_NA_N}$ dissociative character,[47] with a very loose transition state, and limited nucleophilic assistance, as shown by the low hydroxide ion dependence and the small effect of Ln^{3+} radii on rate constants, k_1. This mechanism differs from that proposed for hydrolysis of phosphate monoesters catalyzed by transition metals where association with an aquo complex is important and there is significant water attack on phosphorus. There is probably little charge transfer between the Ln^{3+} and 8QP, although it is important in transition-metal complexes. Quantum mechanical calculations were performed on the catalytic mechanism for hydrolysis of 8QP to test these conclusions.

Computational Studies. Probable reaction paths for the 8QP hydrolysis in the absence and presence of Ln^{3+} were modeled with the $[8QP\cdot(H_2O)_3]^{2-}$ and $[Ln\cdot8QP\cdot(H_2O)_6]^{+}$ structures,

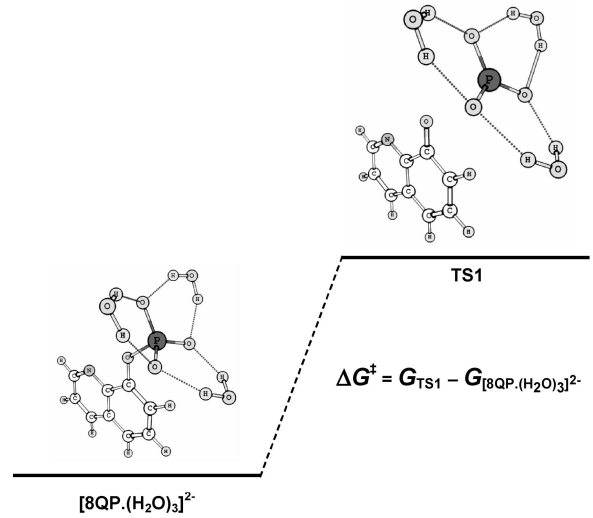

FIGURE 9. Dissociative reaction coordinates for reaction of 8QP in the absence of Ln^{3+}. Structures were optimized at the B3LYP level with basis sets O, N, and P (6-31+G*); C (6-31G*) and H (6-31G).

whose numbering schemes are as in **2** and **3**, i.e., Gibbs free energies of reaction and activation are compared for $[8QP\cdot(H_2O)_3]^{2-}$ and $[Ln\cdot8QP\cdot(H_2O)_6]^{+}$. Figures 9 and 10 represent optimized reaction coordinates for the dissociative mechanism of 8QP in the absence and presence of lanthanide ions, respectively. Tables 4 and 5 include some selected geometric parameters for reactants and the transition states without and with Ln^{3+}, respectively.

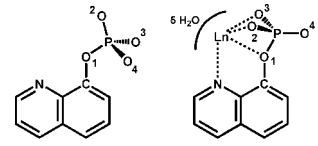

2 **3**

The reaction coordinate for the reaction of $8QP^{2-}$ was modeled by the $[8QP\cdot(H_2O)_3]^{2-}$ structure because gas-phase $8QP^{2-}$ has a bond length P−O1 of 2.015 Å, which is ∼0.3 Å longer than for phosphate monoester dianions in the solid state (∼1.7 Å).[48] This difference is general for calculated structures of gas-phase monoester phosphate dianions, which relates their dissociation to the stability of the gas-phase metaphosphate anion.[49] Thus, inclusion of solvent effects is essential, by a polarizable continuum method (PCM-type approach), or by adding a few water molecules (explicit solvation) for hydration of polar and ionic groups,[50,51] i.e., the phosphoryl oxygen atoms. Both approaches are limited, because PCM neglects specific interactions of water molecules with the phosphoryl group[52] and explicit solvation should consider fluctuations with averaging over large numbers of water molecules and of accessible configurations,[53] which is very demanding and involves the interaction potential between solute and solvent.

(44) Choppin, G. R.; Bünzli, J.-C. G. *Lanthanide probes in life, chemical and earth sciences - Theory and practice*; Elsevier: Amsterdam, 1989; pp 1−41.
(45) Kodama, M.; Koike, T.; Mahatma, A. B.; Kimura, E. *Inorg. Chem.* **1991**, *30*, 1270–1273.
(46) Murakami, Y.; Sunamoto, J.; Sadamori, H. *J. Chem. Soc., Chem. Commun.* **1969**, 983–984.
(47) Kirby, A. J.; Varvoglis, A. G. *J. Am. Chem. Soc.* **1967**, *89*, 415–423.
(48) Jones, P. G.; Kirby, A. J. *J. Am. Chem. Soc.* **1984**, *106*, 6207–6212.
(49) Henchman, M.; Viggiano, A. A.; Paulson, J. F.; Freedam, A.; Wormhoudt, J. *J. Am. Chem. Soc.* **1985**, *107*, 1453–1455.
(50) Wang, Y.-N.; Topol, I. A.; Collins, J. R.; Burt, S. K. *J. Am. Chem. Soc.* **2003**, *125*, 13265–13273.
(51) Kirby, A. J.; Dubba-Roy, N.; Silva, D.; Goodman, J. M.; Lima, M. F.; Roussev, C. D.; Nome, F. *J. Am. Chem. Soc.* **2005**, *127*, 7033–7040.
(52) Cramer, C. J.; Truhlar, D. G. *Chem. Rev.* **1999**, *99*, 2161–2200.
(53) Åqvist, J.; Kolmodin, K.; Florian, J.; Warshel, A. *Chem. Biol.* **1999**, *6*, R71–R80.

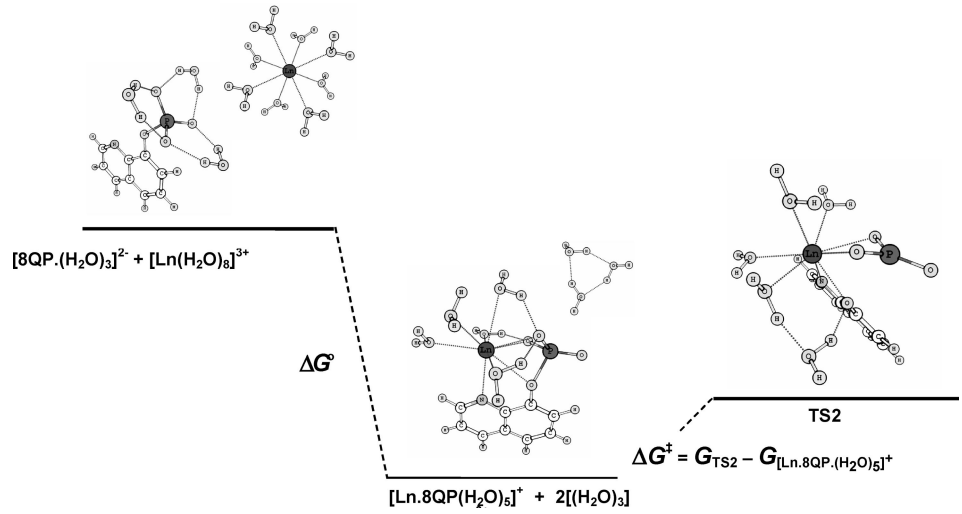

FIGURE 10. Dissociative reaction coordinates for reaction of 8QP in the presence of Ln^{3+}. Structures of the lanthanide complexes are similar and only those with La^{3+} are shown. Structures were optimized at the B3LYP level by using the following basis sets: La^{3+} (ECP46MWB); Sm^{3+} (ECP51MWB); Tb^{3+} (ECP54MWB); Er^{3+} (ECP57MWB); O, N, and P (6-31+G*); C (6-31G*), and H (6-31G).

TABLE 4. Selected Distances (Å) and Angles (deg) for Optimized Structures of $8QP^{2-}$, $[8QP(H_2O)_3]^{2-}$, and TS1[a]

	$8QP^{2-}$	$[8QP(H_2O)_3]^{2-}$	TS1
C−O1	1.287	1.317	1.262
P−O1	2.015	1.796	3.455
P−O2	1.522	1.531	1.509
P−O3	1.530	1.540	1.510
P−O4	1.529	1.541	1.510
O2−P−O3	118.2	116.1	119.8
O2−P−O4	118.2	116.1	119.8
O3−P−O4	116.4	114.5	119.5

[a] B3LYP calculations with basis sets: O, N, and P (6-31+G*), C (6-31G*), and H (6-31G).

We consider explicit solvation with a few water molecules, mainly because PCM-type approaches have not been fully tested and validated for lanthanide complexes. Also, in order to avoid many local minima on the potential energy surface (PES), only three water molecules were explicitly added in hydration of the phosphoryl oxygens of $8QP^{2-}$, establishing the $[8QP\cdot(H_2O)_3]^{2-}$ complex with a C_s symmetry (Figure 9). The calculated P−O1 bond length of 1.796 Å is consistent with that in solution, being less than 0.1 Å longer than in the solid, where packing forces and the absence of explicit hydration shorten bonds.

With lanthanide ions, reaction path calculations were performed on the $[Ln\cdot 8QP(H_2O)_6]^{+}$ complexes (Figure 10), which were selected from optimizations of the $[8QP\cdot(H_2O)_3]^{2-}$ and $[Ln(H_2O)_8]^{3+}$ systems leading to $[Ln\cdot 8QP(H_2O)_5]^{+} + 2[H_2O]_3$ (clusters). Initial structures of these complexes were created by coordination at the probable sites of 8QP, namely, of the quinolinic nitrogen and phosphoryl oxygens to Ln^{3+} and by placing water molecules at ca. 2.5 Å from Ln^{3+} to complete coordination numbers of 8 or 9, typical for lanthanide ions.

As shown in Table 5, the main effects of Ln^{3+} complexation are on the structure of the phosphate group. Bond lengths change slightly from La^{3+} to Er^{3+}, with 0.009 Å shortening of the P−O1 bond, and there are evident changes in the bond angles, mainly O2−P−O3, which in the complexes are about 12° smaller than in $[8QP(H_2O)_3]^{2-}$. There is also a gradual decrease of 1.3° in the O2−P−O3 angles with decreasing lanthanide radii. Changes in angles are energetically much less demanding than in bond length.

The equilibria in Scheme 3 and Figure 10 are markedly displaced toward formation of the $[Ln\cdot 8QP(H_2O)_5]^{+}$ complexes, $\Delta G^\circ \approx -2000$ kJ mol^{-1}, due to the strong bond with Ln^{3+}, the charge decrease, and the small $Ln-OH_2$ bond energies. We note that in this model, a few water molecules provide the solvation, so that major differences relative to the aqueous phase are mainly due to the last two factors, which are reduced by the solvent. Thus, for comparison, effects on the charge, and partially on the $Ln-OH_2$ bond energies, are reduced by scaling to La^{3+}. As a result, for Sm^{3+}, $\Delta\Delta G^\circ = (\Delta G^\circ_{Sm} - \Delta G^\circ_{La}) = -28.4$ kJ mol^{-1}, which decreases toward Er^{3+}, namely, $\Delta\Delta G^\circ = -45.5$ kJ mol^{-1}. This scaling yields a trend that to some extent follows the experimental data (Table 6).

The reaction coordinate from ground state, $[8QP(H_2O)_3]^{2-}$, to TS1 is indicative of a very loose transition state with O−P−O angles near to 120° and a P−O1 bond longer by 1.665 Å and of C−O1 shorter by 0.111 Å. The calculated activation Gibbs energy, $\Delta G^\ddagger = 57.3$ kJ mol^{-1}, is typical of a gas phase reaction and is lower than in solution with no desolvation, solvent reorganization and differential solvation between ground and transition states. For example, the hydrolysis of *p*-nitrophenyl phosphate dianion has $\Delta G^\ddagger = 124$ kJ mol^{-1} at 25 °C in water, but in DMSO/H_2O 95:5, it decreases to 93.6 kJ mol^{-1}, mainly due to partial desolvation of the phosphoryl group.[54] A similar argument can be made for the calculated values of $\Delta G^\ddagger$ for reactions in the presence of Ln^{3+}, which are systematically smaller than those calculated from values of k_1 at pH = 7.00. The behavior of TS2 differs from that of TS1 relative to their respective ground states, for example, the P−O1 bond length is longer in TS1 by about 1.7 Å, but 0.8 Å in TS2 (0.809 Å to La^{3+} and 0.774 Å to Sm^{3+}). This observation indicates a stronger P−O1 bond, and the putative metaphosphate ions in TS2 are practically planar and loose, but with distorted O−P−O bond angles, namely, ∼108° and ∼126°, which are ∼6° and ∼3° larger than in the ground state. In structure **1**, HO^- coordinated to La is shown as attacking phosphorus, as in dephosphorylations by H_2O/HO^- complexed to a transition metal ion. In this respect, we note that TS2 is consistent with a single step $\mathbf{D_NA_N}$ mechanism with a rather loose transition state, where the planar

(54) Grzyska, P. K.; Czyryca, P. G.; Golightly, J.; Small, K.; Larsen, P.; Hoff, R. H.; Hengge, A. C. *J. Org. Chem.* **2002**, *67*, 1214–1220.

TABLE 5. Selected Atomic Distances (Å), Angles (deg), and Dihedral Angles (deg) for Optimized Structures of $[Ln\cdot 8QP(H_2O)_5]^+$ and TS2[a]

	$[Ln\cdot 8QP(H_2O)_5]^+$				TS2		
	La	Sm	Tb	Er	La	Sm	Tb
C−O1	1.374	1.374	1.373	1.373	1.353	1.353	1.354
P−O1	1.784	1.780	1.781	1.777	2.574	2.545	2.512
P−O2	1.579	1.579	1.578	1.580	1.534	1.533	1.534
P−O3	1.569	1.570	1.571	1.573	1.531	1.534	1.535
P−O4	1.475	1.475	1.474	1.473	1.470	1.470	1.470
Ln−O1	2.615	2.555	2.526	2.517	2.392	2.318	2.283
Ln−O2	2.563	2.478	2.418	2.364	2.592	2.521	2.480
Ln−O3	2.461	2.383	2.356	2.325	2.593	2.490	2.443
Ln−N	2.681	2.594	2.552	2.513	2.642	2.550	2.506
O2−P−O3	102.5	102.0	101.6	101.2	108.2	107.7	107.4
O2−P−O4	123.8	124.2	124.5	124.6	125.6	126.0	126.2
O3−P−O4	123.4	123.5	123.7	123.8	125.9	126.0	126.1
C−O1−Ln−N	22.2	22.8	23.4	23.8	10.5	9.5	8.3

[a] B3LYP calculations with basis sets: La^{3+} (ECP46MWB), Sm^{3+} (ECP51MWB), Tb^{3+} (ECP54MWB), Er^{3+} (ECP57MWB), O, N, and P (6-31+G*), C (6-31G*), and H (6-31G).

TABLE 6. B3LYP/ECP Gibbs Energy of Reaction and of Activation, Enthalpy and Entropy of Activation, Experimental Gibbs Energies, And Relative Gibbs Energies Associated with Structures in Figures 9 (Absence of Ln^{3+}) and 10 (Presence of Ln^{3+})[a]

	TS1	La	Sm	Tb	Er
$\Delta\Delta G^\circ$ (B3LYP)[b]		0	−28.4	−39.0	−45.5
$\Delta H^\ddagger$ (B3LYP)	79.2	28.3	19.9	14.3	
$T\Delta S^\ddagger$ (B3LYP)	21.9	6.7	6.3	5.9	
$\Delta G^\ddagger$ (B3LYP)	57.3	21.6	13.6	8.3	5.5[c]
$\Delta\Delta G^\ddagger$ (B3LYP)[d]	0	35.7	43.7	49.0	51.8
$\Delta G^\ddagger$ (exp)[e]	126.2	91.6	88.9	90.3	91.1
$\Delta\Delta G^\ddagger$ (exp)[d]	0	34.6	37.3	35.9	35.1
$\Delta\Delta G^\circ$ (exp)[b,f]		0	−1.03	−1.94	−2.28
$\Delta_{hyd}\Delta G^{\ddagger}$[g]	68.9	70.0	75.3	82.0	85.6

[a] All quantities calculated at 298.15 K and expressed in kJ mol^{-1}. B3LYP calculations with the following ECPs and basis sets: La^{3+} (ECP46MWB), Sm^{3+} (ECP51MWB), Tb^{3+} (ECP54MWB), Er^{3+} (ECP57MWB), O, N, and P (6-31+G*), C (6-31G*), and H (6-31G)). [b] $\Delta\Delta G^\circ = \Delta G^\circ_{Ln} - \Delta G^\circ_{La}$. [c] Estimated from the linear relationship between $\Delta G^\ddagger$ (B3LYP) and Ln^{3+} radii. [d] $\Delta\Delta G^\ddagger = \Delta G^\ddagger(TS1) - \Delta G^\ddagger(TS2)$. [e] Estimated from $\Delta G^\ddagger = RT\ \ln[(k_BT)/(hk_1)]$, with k_B and h being the Boltzmann and Planck constants, respectively, and k_1 was taken from Table 1 at pH = 7.00, and T is the temperature. [f] Calculated from $\Delta G^\circ = -RT\ln K^\circ_{QP}$. [g] Calculated as $\Delta G^\ddagger(exp) - \Delta G^\ddagger(B3LYP)$.

PO_3^- would allow limited "association" with a water molecule not included in the reaction scheme. Here the distinction between "associative" and "dissociative" is essentially one of timing. Computation indicates extensive formation of PO_3^- in the transition state, but it is not evident from experiment and a single step $\mathbf{D_NA_N}$ is the most probable mechanism.

The B3LYP calculated values of $\Delta G^\ddagger$ for the gas phase indicate that these reactions are strongly favored by lanthanide ions with decreasing activation Gibbs energies from 56.9 kJ mol^{-1} in their absence to 21.6, 14.6, and 8.3 kJ mol^{-1} in the presence of La^{3+}, Sm^{3+}, and Tb^{3+}, respectively. These calculated values are largely independent of the basis sets used for the P atom. The following changes of $\Delta G^\ddagger$ are calculated: 56.9, 57.3, and 59.9 kJ mol^{-1} with the 6-31G*, 6-31+G*, and 6-311+G(3df) basis sets, respectively, in the absence of Ln^{3+} and 21.7, 21.6, and 26.7 kJ mol^{-1} in the presence of La^{3+} (Supporting Information, Table S16). We note that the lanthanide ions energetically favor the reaction with significant decreases of the activation enthalpy, whereas the entropic contributions become less favorable with Ln^{3+}. This conclusion is reasonable probably because the PO_3^- moiety can coordinate to the lanthanide ion, thus making TS2 more compact than TS1, which decreases the entropy difference between transition states and reactants. However, despite this less favorable entropic contribution, calculated Gibbs energies indicate the strong catalytic effects of Ln^{3+}. There is a correlation between calculated values of $\Delta G^\ddagger$ and the ionic radii of Ln^{3+}, namely, $\Delta G^\ddagger$ decreases linearly as a function of decrease in the Ln^{3+} radius (Supporting Information, Figure S4), and when this linear relationship is extrapolated to the Er^{3+} radius a $\Delta G^\ddagger = 5.5$ kJ mol^{-1} is predicted, hence the difficulties in describing TS2 for this ion.

Although B3LYP-calculated values of $\Delta G^\ddagger$ are much smaller than those estimated from k_1, it is clear from Table 6 that differences are mainly due to hydration effects which are not included in the B3LYP calculations. The semiquantitative trends observed for the hydrolysis in absence and in the presence of Ln^{3+} are quite well reproduced by the calculations. In addition, the estimated hydration effects from the difference between the experimental and calculated values of $\Delta G^\ddagger$ follow a systematic increase with the decrease of the Ln^{3+} radii, consistent with the increase of charge densities of the ions. These comparisons between the calculated and experimental values of $\Delta G^\ddagger$ support the qualitative results and conclusions obtained from the B3LYP calculated properties.

Analyzing the effects of Ln^{3+} in the ground states shows that there is an increase in the C−O1−Ln−N dihedral angle from La^{3+} to Er^{3+}, which is opposite to the trends in the transition states. Such behavior indicates that lanthanide ions with smaller radii should interact favorably with N and O1 atoms during leaving group departure. Because catalysis proceeds without an increase in the P−O1 bond length, it seems that electronic, rather than structural effects, are responsible for acceleration of 8QP hydrolysis, and atomic partial charges were estimated with the ChelpG method for the optimized structures (Table 7). Formation of a complex with Ln demonstrates the decrease of initial state free energy.

Differences in atomic charges in the ground ($[8QP(H_2O)_3]^{2-}$) and transition states (TS1) of the uncatalyzed reaction indicate a largely dissociative mechanism, with decrease of the partial positive charge on P and the O1 atom becoming more negative with metaphosphate and aryloxide ion formation.

Despite postulated electronic effects of Ln^{3+}, partial atomic charges in ground and transition states, TS2 and TS1 of catalyzed and uncatalyzed reactions, are unexpectedly similar and vary on P and O1 atoms by only ∼0.04*e* and ∼0.17*e*, respectively, even though, P−O1 bond lengths change by ∼0.8 and ∼1.7 Å, respectively. In addition, while P−O1 bond lengths

TABLE 7. ChelpG Atomic Partial Charges at the B3LYP/ECP Level for $[8QP(H_2O)_3]^{2-}$, $[Ln\cdot 8QP(H_2O)_5]^{+}$, and Its Respective Transition States, TS1 and TS2[a]

	$[8QP(H_2O)_3]^{2-}$		$[Ln\cdot 8QP(H_2O)_5]^{+}$					
	GS	TS	La	Sm	Tb	Er	TS2 (La)	TS2 (Sm)
P	1.23	1.17	1.40	1.40	1.40	1.39	1.38	1.37
C	0.32	0.38	0.09	0.03	0.01	0.03	0.18	0.20
N	−0.63	−0.69	−1.04	−1.03	−1.01	−1.01	−0.88	−0.90
O1	−0.42	−0.62	−0.60	−0.58	−0.54	−0.54	−0.74	−0.75
O2	−0.84	−0.67	−0.86	−0.86	−0.86	−0.87	−0.83	−0.82
O3	−0.84	−0.68	−0.91	−0.93	−0.93	−0.95	−0.86	−0.85
O4	−0.84	−0.68	−0.65	−0.64	−0.63	−0.63	−0.56	−0.56
Ln	−	−	2.57	2.53	2.45	2.45	2.58	2.55

[a] ECPs and basis sets: La^{3+} (ECP46MWB), Sm^{3+} (ECP51MWB), Tb^{3+} (ECP54MWB), Er^{3+} (ECP57MWB), O and N (6-31+G*), C and P (6-31G*), and H (6-31G).

in $[8QP(H_2O)_3]^{2-}$ and $[8QP\cdot Ln(H_2O)_5]^{+}$ complexes are similar, 1.80 and 1.78 Å, respectively, ChelpG charges are $P^{+1.23}-O^{-0.42}$ and $P^{+1.40}-O^{-0.60}$, respectively, indicating increased polarization. This difference could indicate a higher stability of structure **4** relative to **5**, indicating that lanthanide ions favor leaving group departure in a loose transition state, which is consistent with a single step $\mathbf{D_NA_N}$ mechanism. However, we note that partial atomic charges are only as reliable as the energies calculated with DFT. Thus, caution should be exercised when using atomic charges to interpret reaction mechanisms, and other electronic quantities should also be used.

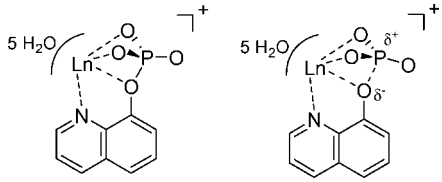

4 **5**

Lanthanide ions increase the P−O1 bond polarization bringing the electronic structure of the reactant (ground state) closer to that of the transition state for P−O1 dissociation (in hydrolysis) and, in addition to this polarization, coordination of Ln^{3+} to O1 decreases the C−O1 bond order. Wiberg bond indexes on the natural atomic orbital (NAO) basis are 1.17 and 0.97, consistent with the overlap-weighted NAO bond orders: 0.94 and 0.80 for $[8QP(H_2O)_3]^{2-}$ and $[8QP\cdot La(H_2O)_5]^{+}$ complexes. These results favor structure **5**, where the metaphosphate ion is stabilized, which is close to a transition state in a $\mathbf{D_NA_N}$ type dissociative mechanism. The similarities of structure **5** and the transition state, induced by Ln^{3+}, is also shown by the decreasing C−O1 bond distance which decreases by only ∼0.02 Å (1.37 Å × 1.35 Å) from the ground state to TS2 in the $[8QP\cdot Ln(H_2O)_5]^{+}$ complex.

The coordination of PO_3^- to the Ln^{3+} ion changes the features of the ground and transition states, because without lanthanide ion the interaction of the PO_3^- with water is significant (see Figures 9 and 10), whereas upon coordination, these interactions lose their importance (see Figure 10), which considerably alters the reaction paths.

The reaction paths involving a direct water attack on the P atom, without and with the presence of the lanthanide ion, have also been explored by the same computational approach. The model systems used differ slightly from those presented in Figures 9 and 10 by the presence of one additional hydration water molecule, which will be responsible for the attack. The reaction coordinates for these associative paths are illustrated in Figures S5 and S6 in the Supporting Information.

It is clear that the reaction paths involving the direct attack of the water molecule in the absence and presence of La^{3+} are highly energetic and, are thus, unfavored compared to the dissociative paths presented in Figures 9 and 10. In addition, the reaction profiles illustrated in Figures S5 and S6 (Supporting Information) are very steep, which make determination of the transition-state structures very difficult, and even after more than 20 attempts such determinations were unsuccessful. However, despite the lack of these transition-state structures, given the large energetic differences between these reaction paths and the dissociative ones (Figures 9 and 10), the former would be disallowed. In order to avoid comparison between different model systems (Figure 9 and Figure S4, Supporting Information), the dissociative reaction profile P−O1 has been calculated with the structure in Figure 9 with one additional water molecule. The energy maximum in this P−O1 reaction coordinate is ∼90 kJ mol^{-1} (Supporting Information, Figure S7) and is significantly lower that that found in Figure 9 (∼270 kJ mol^{-1}) and very similar to $\Delta H^{\ddagger}$ (79.2 kJ mol^{-1}) in Table 6, thus validating the previous statement.

Conclusions

Hydrolysis of 8-quinolyl phosphate (8QP) in the presence of trivalent lanthanides (Ln = La, Sm, Eu, Tb, and Er) proceed through formation of an $[Ln\cdot 8QP]^{+}$ complex that decomposes into products. The computational studies indicate that there is significant P−O1 bond breaking in the transition state, a result consistent with the fact that phosphate monoesters dianions show a flat potential energy surface and that the transition state changes from associative to dissociative upon decrease in the pK_a of the leaving group.[11] The theoretical results were fundamental in facilitating understanding of the mechanistic results, especially because kinetics, activation parameters and isotope effects did not allow a conclusive distinction between associative and dissociative mechanisms. Apparently, formation of the $[Ln\cdot 8QP]^{+}$ complex alters electron distribution and effectively lowers the pK_a of the leaving group, favoring the dissociative pathway. The reactions exhibit more than 10^7-fold rate enhancements, which B3LYP calculations indicate are driven by leaving group and metaphosphate stabilization in a single step $\mathbf{D_NA_N}$-type dissociative mechanism, consistent with limited nucleophilic assistance, as shown by the low hydroxide ion dependence and the small effects of Ln^{3+} radii on rate constants, k_1.

Experimental Section

Materials. Inorganic salts, buffers, and 8-hydroxyquinoline (8QOH), analytical grade, were used without further purification. Bis-tris-propane (BTP) and hydrated lanthanide chlorides ($LnCl_3 \cdot xH_2O$), >99% purity, were used as received. Solvents were dried over drying agents and distilled before use. Distilled, deionized water was used in all studies, and CO_2 was removed by boiling. ^1H and ^{31}P NMR spectra were recorded at 200 and 81 MHz, respectively, in D_2O with sodium 3-(trimethylsilyl)propionate (TSP) as internal reference for ^1H NMR and 85% phosphoric acid as external reference for ^{31}P NMR spectra.

Synthesis of Quinolinium-8-yl Hydrogen Phosphate (8-Quinolyl Phosphate, Zwitterion Form).[29,30] A solution of PCl_5 (718 mg, 3.45 mmols) in $CHCl_3$ (15 mL) was added dropwise to 8QOH (500 mg, 3.45 mmol in $CHCl_3$, 15 mL) in an ice−water bath. The mixture was stirred at room temperature for 60 min. Water was then added (~3 equiv) and the mixture left to react overnight. The solvent was removed under reduced pressure, and acetone (10 mL) and water (3 mL) were added to the crude oil. Pale fine crystals formed slowly and were collected by filtration and acetone washed to give313 mg (40%, mp 200−202 °C dec). Results of ^1H and ^{31}P NMR spectroscopy are consistent with a sample with purity >99%. At pD = 2.15 in D_2O, the following signals were observed: ^{31}P NMR δ 3.72 ppm; ^1H NMR δ 7.86 (dd, 1H, J_{56} = 6.7 Hz and J_{67} = 7.8 Hz), δ 7.96 (d, 2H), δ 8.08 (dd, 1H, J_{23} = 7.1 Hz and J_{34} = 5.6 Hz), δ 9.09 (d, 1H, J_{34} = 5.6 Hz) and δ 9.12 ppm (d, 1H, J_{23} = 7.1 Hz).

Kinetics and Products. ATR-FTIR Studies. Reactions were monitored at 25 ± 2 °C on a spectrometer with a MCT detector, and a CIRCLE cell (Spectra Tech) mounted with a ZnSe crystal, 10 cm path length. Parameters were set to 10.0 Å aperture, automatic gain and 0.20 cm s^{-1} scan rate. Each spectrum was recorded in the 800−4000 cm^{-1} range with spectral resolution, 1.0 cm^{-1}, and is the result of 64 interferograms. Reactions were started by addition of 200 μL of 0.05 M stock aqueous solutions of 8QP or K_2HPO_4 into 10.0 mL of reaction mixture.

UV−vis Spectrophotometry. Buffered solutions were prepared by addition of aqueous standard HCl (0.1M; Merck) to aqueous BTP (0.01 M), and the pH of each reaction mixture was measured at the beginning and end of each run. Hydrolysis of 8QP in the presence of the Ln^{3+} were followed by monitoring the lanthanide 8-quinolinolate complex, $[Ln \cdot 8QO]^{2+}$, at 257 nm and 25.0 °C in quartz cuvettes controlled with a thermostated water-jacketed cell holder. Reactions were started by injection of 10 μL of 10 mM stock solutions of 8QP in water (pH ~ 10 and stored in a refrigerator to minimize hydrolysis) into 3 mL of aqueous 0.01 M BTP giving 33.3 μM 8QP. Absorbance versus time data (at least 90% reaction) were stored directly on a microcomputer. First-order rate constants, k_{obs}, were estimated from linear plots of $\ln(A_\infty - A_t)$ against time, except when $[La^{3+}]/[8QP] < 40$, where reactions were consecutive and rate constants were estimated from eq 6

$$A_t = \left\{1 + \frac{k_a e^{-k_1 t} - k_1 e^{-k_a t}}{k_1 - k_a}\right\} A_\infty \qquad (6)$$

where k_a is the rate constant for formation of the [8QO·La] complex, with $k_a \neq k_1 \gg$ rate constant for reversion of [8QO·La] to reagents. All correlation coefficients were >0.996, as estimated by iterative least-squares fits.

Potentiometric Titration. The pK_a values of 8QP were determined with a digital pH meter and a combined glass electrode. Titrations were in a 150-mL thermostatted cell, under N_2 at 25.0 °C, ionic strength 0.1 M, KCl, and 1.0 mM initial 8QP. The solution was titrated with small increments of 0.1008 M KOH, CO_2-free, and precautions were taken to eliminate carbonate and CO_2 during the titration. The program BEST7[32] was used to calculate the dissociation constants.

Spectrophotometric pH Titration. Absorbances were monitored on a diode-array spectrophotometer with a thermostatted cell holder at 25.0 °C with 33.3 μM of 8QP with 0.01 M buffer: HCOOH (pH 3−4.5); CH_3COOH (pH 4−5.5); NaH_2PO_4 (pH 5.5−7.8); H_3BO_3 (pH 7.8−9.0).

NMR titration was at 25.0 °C. The 8QP solution (10 mg/mL) was titrated with NaOD with $pD = pH_{read} + 0.4$.[55]

Calculations were performed with Gaussian 98[56] at the DFT level, with the B3LYP functional.[57,58] Defaults for convergence and optimization were used without any symmetry constraints. The $46 + 4f^N$ electrons of Ln^{3+} were treated as core electrons (MWB46 La^{3+}, MWB51 Sm^{3+}, MWB54 Tb^{3+}, and MWB57 Er^{3+}) described by the effective core potential (ECP) of Dolg et al.[59] which describes the valence electrons by the contracted basis sets (7s6p5d)/[5s4p3d]. The N, O, and P atoms were described by the 6-31+G* basis sets and C and H by 6-31G* and 6-31G basis sets, respectively.[60,61]

The initial conformation of $8QP^{2-}$ without lanthanide was obtained conventionally. With a lanthanide, initial structures of the complexes were based on coordination numbers of 8 and 9, as probable binding sites of 8QP, the quinolinic nitrogen and phosphate oxygen atoms. Water molecules and other ligands were positioned at a distance of ca. 2.5 Å from the metal. The critical points in the Potential Energy Surface (PES), namely, reactants, products, intermediates and transition states, were properly characterized by their force constants, which were all positive, except for the transition state with its imaginary frequency. The transition states were found through a continuous structural search on the PES and then optimized by using an eigenvalue-following algorithm. The charges were obtained with fully optimized structures and the ChelpG procedure,[62] with lanthanide radii of La^{3+} 1.216, Sm^{3+} 1.132, Tb^{3+} 1.095 and Er^{3+} 1.062 Å.[41] The natural orbital analysis for the La^{3+} complexes was performed with the WMB28 ECP basis set.[59]

Acknowledgment. We dedicate this paper to Prof. Francisco Carlos Nart (in memoriam), and we acknowledge the Brazilian agencies FUNCITEC (PRONEX) and CNPq for their financial support and the Office of International Programs, NSF.

Supporting Information Available: Potentiometric titration of 8QP, Cartesian coordinates of the B3LYP-optimized structures, and the energy profile for the associative and dissociative path containing four water molecules. This material is available free of charge via the Internet at http://pubs.acs.org.

JO801870V

(55) Schowen, K. B. J. *Transition States of Biochemical Processes*; Springer: New York, 1978; pp 225−284.
(56) Frisch, M. J.; Trucks, G. W.; Schlegel, H. B.; Scuseria, G. E.; Robb, M. A.; Cheeseman, J. R.; Zakrzewski, V. G.; Montgomery, J. A., Jr.; Stratmann, R. E.; Burant, J. C.; Dapprich, S.; Millam, J. M.; Daniels, A. D.; Kudin, K. N.; Strain, M. C.; Farkas, O.; Tomasi, J.; Barone, V.; Cossi, M.; Cammi, R.; Mennucci, B.; Pomelli, C.; Adamo, C.; Clifford, S.; Ochterski, J.; Petersson, G. A.; Ayala, P. Y.; Cui, Q.; Morokuma, K.; Malick, D. K.; Rabuck, A. D.; Raghavachari, K.; Foresman, J. B.; Cioslowski, J.; Ortiz, J. V.; Stefanov, B. B.; Liu, G.; Liashenko, A.; Piskorz, P.; Komaromi, I.; Gomperts, R.; Martin, R. L.; Fox, D. J.; Keith, T.; Al-Laham, M. A.; Peng, C. Y.; Nanayakkara, A.; Gonzalez, C.; Challacombe, M.; Gill, P. M. W.; Johnson, B. G.; Chen, W.; Wong, M. W.; Andres, J. L.; Head-Gordon, M.; Replogle, E. S.; Pople, J. A. *Gaussian 98*, revision A.6; Gaussian, Inc.: Pittsburgh, PA, 1998.
(57) Becke, A. D. *J. Chem. Phys.* **1993**, *98*, 5648–5652.
(58) Lee, C.; Yang, W.; Parr, R. G. *Phys. Rev. B* **1988**, *37*, 785–789.
(59) Dolg, M.; Stoll, H.; Savin, A.; Preuss, H. *Theor. Chim. Acta* **1989**, *75*, 173–194.
(60) Ditchfield, R.; Hehre, W. J.; Pople, J. A. *J. Chem. Phys.* **1971**, *54*, 724–728.
(61) Hehre, W. J.; Ditchfield, R.; Pople, J. A. *J. Chem. Phys.* **1972**, *56*, 2257–2261.
(62) Breneman, C. M.; Wiberg, K. B. *J. Comput. Chem.* **1990**, *11*, 361–373.